low temperatures, holes tend to congregate in these directions.

If this conjecture is correct, the change in modulus for the heavy-hole surface should follow that for germanium, as given by Eq. (12), while that for the light-hole surface should follow Eq. (8) with kT replaced by (10), for the low temperatures, giving

$$\Delta c_{11_0} = -\frac{16}{3}\left(\frac{\pi}{3}\right)^{2/3} \frac{m^* N^{1/3} \Phi^2}{h^2}. \quad (31)$$

If we take an average value of 15 eV for the shear deformation potential d, the indicated change in modulus from Eq. (12)—using $m^* = 0.49 m_0$ and $N = 0.85 N_0$, i.e., 2.12×10^{18} heavy holes—is 26.5×10^9 dyn/cm^2, which is not out of line with the values of Fig. 8(b) extrapolated to lower temperatures. For higher doping levels this effect disappears since the momentum differences for the various positions become smaller.

Another piece of evidence that the light holes congregate along ⟨100⟩ positions at low temperatures is furnished by the nearly constant relaxation time of Fig. 11 for longitudinal waves propagated along the ⟨100⟩ direction. The data of Fig. 12 show that p-silicon with boron becomes degenerate for a doping of 3×10^{19} atoms per cc. This is taken to mean that the impurities are near enough together to prevent any excited state orbits around the boron atoms. The smallest orbits will be executed by the heavy holes and hence they will reach degeneracy at a higher doping level than the light hole surface. With a mass ratio of 0.49 to 0.16 or 3.06, the radius will be this factor larger for the light-hole surface. Hence, this surface should become degenerate for a doping of

$$3 \times 10^{19}/(3.06)^3 \doteq 10^{18} \text{ boron atoms per cc.} \quad (32)$$

Therefore, the constant relaxation time of 4.2×10^{-12} sec for a sample doped with 2.5×10^{18} boron atoms per cc is a confirmation that, at low temperatures, a longitudinal stress along the ⟨100⟩ axis actuates mostly light holes.

If the relaxation time is due to scattering of light holes by impurities, calculations indicate that the scattering radius is about 5×10^{-8} cm, in good agreement with the value obtained for the degenerate heavy-hole surface.

PHYSICAL REVIEW VOLUME 134, NUMBER 5A 1 JUNE 1964

Distribution Functions for the Number of Distinct Sites Visited in a Random Walk on Cubic Lattices: Relation to Defect Annealing*

J. R. BEELER, JR.
Nuclear Materials and Propulsion Operation, General Electric Company, Cincinnati, Ohio
(Received 17 January 1964)

Distribution functions for the number of distinct sites $S(n)$ visited by a point defect executing a symmetric random walk of n jumps on two- and three-dimensional lattices were computed using the Monte Carlo method. The square planar, simple cubic, bcc, and fcc lattices were treated. In three dimensions, the normal distribution appears to describe $S(n)$ for $n > 10^4$ jumps and at 10^4 jumps the derivative $d\bar{S}(n)/dn$ of the average number, $\bar{S}(n)$, of distinct sites is within 0.5% of the value given by Vineyard's exact asymptotic solution. The defect annealing rate was computed using the $S(n)$ distribution in a simple example and this result compared with an analog Monte Carlo solution. The comparison indicated that fluctuations in the initial defect concentration must be considered in computing the initial annealing rate and the mobile defect concentration as a function of time. After 500 jumps the annealing rate, but not the concentration, can be closely approximated without accounting for fluctuations in the initial concentration.

1. INTRODUCTION

IN a monatomic crystal, the migration of a defect, such as a vacancy or an interstitial atom, proceeds as a symmetric random walk[1] on the crystal lattice. The rate at which mobile defects are annihilated or trapped at point sinks is proportional to the rate at which they encounter fresh sites which have not been visited previously. Damask and Dienes[2] will treat the physical side of this process in a forthcoming book. On the basis of a Monte Carlo study, Beeler and Delaney[3] concluded that the average number of distinct sites, $\bar{S}(n)$, visited by a point defect in either a symmetric or an asymmetric random walk of n jumps was of the form,

$$\bar{S}(n) = An^k \quad (1)$$

* Work supported by the U. S. Atomic Energy Commission.

[1] In this discussion a symmetric random walk is one wherein the jump probabilities for each possible jump direction are equal and constant. The vacancy random walk in an alloy is in general asymmetric because of its ordering energy, i.e., the jump probabilities for each possible direction are not equal and also depend upon the position of the vacancy.

[2] A. C. Damask and G. J. Dienes, "Point Defects in Metals" (to be published).

[3] J. R. Beeler, Jr., and J. A. Delaney, Phys. Rev. **130**, 962 (1963); J. R. Beeler, Jr., U.S.A.F. Report ASD-TDR 63-215 (unpublished).

for a two-dimensional lattice, and of the form

$$\bar{S}(n)=B+Cn \tag{2}$$

for a three-dimensional lattice, where A, B, C, and k are constants for a given lattice structure. Their computations pertained to vacancy migration in a binary alloy and describe the relation between $\bar{S}(n)$ and the rate of ordering (disordering) for $n\leq 10^4$ jumps. Migration on the square planar simple cubic, bcc, and fcc lattices was investigated. Vineyard[4] subsequently proved that the asymptotic form of $\bar{S}(n)$ for a three-dimensional symmetric random walk is

$$\lim_{n\to\infty}\bar{S}(n)=Cn. \tag{3}$$

The Monte Carlo results of Beeler and Delaney for $d\bar{S}(n)/dn=C$ on the interval $10^3\leq n\leq 10^4$, in the case of zero ordering energy, agree closely with the exact asymptotic results given by Vineyard's analysis, the Monte Carlo results being about 1% larger than the exact asymptotic values. Vineyard also showed that

$$\bar{S}(n)=(8n)^{1/2}/\pi \tag{4}$$

in one dimension.

In this communication we describe the distribution function $F(S;n)$ for $S(n)$, as given by Monte Carlo calculations, for the square planar (sp), simple cubic (sc), bcc and fcc lattices. $F(S;n)$ is the probability that a defect visits S or less distinct lattice sites in n jumps. Direct application of these distributions to defect annealing calculations is illustrated in a simple, yet physically significant numerical example wherein attention is called to the effect of fluctuations in the initial defect concentration upon the initial defect annealing rate. This effect first came to our attention in a comparison of the annealing rate predicted by $F(S;n)$, on the basis of the macroscopic (average) defect concentration, with that obtained directly in a separate analog Monte Carlo annealing calculation wherein fluctuation effects were automatically accounted for. The presence of fluctuations significantly increased the initial annealing rate relative to that obtained on the basis of the macroscopic concentration.

On the interval $1000<n<5000$, $F(S;n)$ appears to start an approach to the normal distribution. A χ^2 analysis indicated that $F(S;n)$ is very probably normal for $n>10^4$ in three-dimensional lattices, but gives no information on the convergence to a normal distribution in two dimensions. Up to $n=10^4$ the density function $f(S;n)=dF(S;n)/dS$ is definitely skewed to the right. This feature enhances the increased initial annealing rate contribution arising from concentration fluctuations. The indicated increase is possibly large enough to be detectable in high-temperature quenching experiments and should exert a dominant influence during the initial stage of defect annihilation and clustering in irradiated specimens.

[4] G. H. Vineyard, J. Math. Phys. 4, 1191 (1963).

2. COMPUTATIONAL METHOD

Distribution functions $F(S;n)$ and density functions $f(S;n)$ for each lattice were estimated by running 1000 independent random walk histories of 10^4 jumps each using an IBM-7090 computer. The mean ($\bar{S}$), mode (S^*), median (S_m) and standard deviation (σ) were computed at 10-jump intervals up to 100 jumps, 100-jump intervals up to 10^3 jumps, and 1000-jump intervals up to 10^4 jumps. In each instance an expected tendency toward the normal distribution was monitored by performing an χ^2 test for 21 deg of freedom[5] and computing the coefficients of skewness (γ_1) and excess (γ_2).[6] $\bar{S}(n)$ and σ were computed using the first 500 histories, the second 500 histories and all 1000 histories. The differences between the results given by each sample set were found to be negligible and on this basis we decided that the 1000-history sample size was sufficiently large to form a basis for annealing calculations. In this regard, it is interesting to note that the difference between the present $\bar{S}$ results, based on a least-squares fit to data from 1000 histories, and the original calculations of Beeler and Delaney, based on a least-squares fit to the data from only 10 histories, is less than 0.5%.

3. DISTRIBUTION FUNCTION RESULTS

Selected plots of $F(S;n)$ for $n=10$, 20, 50, 100, 1000, and 10 000 jumps are given in Figs. 1–4 in terms of the ratio $S(n)/n$. This mode of presentation makes it easier to see how $F(S;n)$ changes as n increases, than if the curves were plotted versus $S(n)$. Let $S_1(n)$ be the largest S value such that $F(S;n)=0$ and $S_2(n)$ the smallest S wave such that $F(S;n)=1$. The range of the distribution is defined as $\Delta S(n)=S_2(n)-S_1(n)$. In all instances $\Delta S(n)/n$, $\bar{S}(n)/n$, $S_m(n)/n$, and $S^*(n)/n$ decrease monotonically as n increases. $S_1(n)/n$ remains more or less constant in the two-dimensional case, the diminution in $\Delta S/n$ arising essentially from a monotonic decrease in $S_2(n)/n$. In the three-dimensional

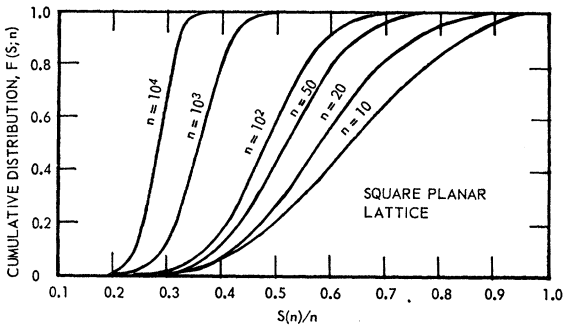

FIG. 1. Distribution function for square planar lattice.

[5] D. R. Evans, *The Atomic Nucleus* (McGraw-Hill Book Company, Inc., New York, 1955); see pp. 774–777.

[6] H. Cramer, *Mathematical Methods of Statistics* (Princeton University Press, Princeton, New Jersey, 1954); see p. 183.

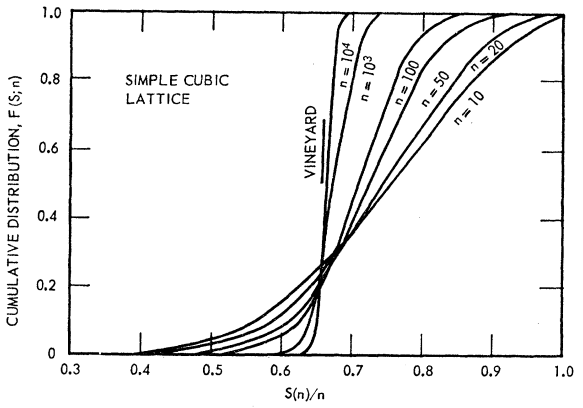

FIG. 2. Distribution function for simple cubic lattice. Vertical tick in Figs. 2–4 indicates Vineyard's asymptotic solution for $S(n)/n$.

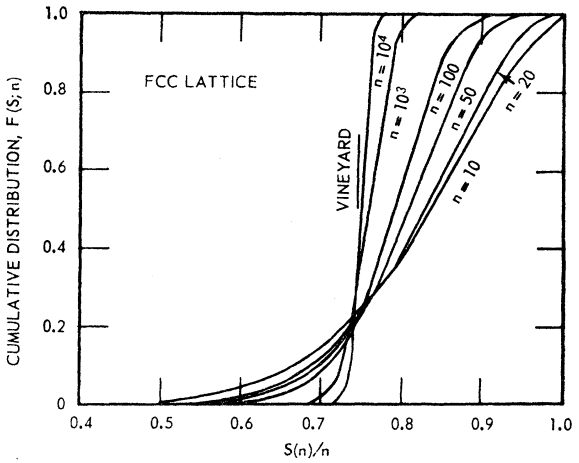

FIG. 4. Distribution function for fcc lattice.

lattices, however, both $S_1(n)/n$ and $S_2(n)/n$ change as n increases, $S_1(n)/n$ tending toward $\bar{S}(n)/n$ from below and $S_2(n)/n$ approaching it from above. The vertical tick defines the lower limit of $\bar{S}(n)/n$ given by Vineyard's calculations for $n\rightarrow\infty$. For all practical purposes, one can consider this asymptotic behavior to be attained at $n=10^4$ jumps. Table I compares the 1000-history Monte Carlo results for $d\bar{S}/dn$ at $n=10^4$ with Vineyard's evaluations for the asymptotic case.

All distributions were skewed negatively for $n\leq 10^4$ as shown by the coefficient of skewness listed in Table II. This skewness is evident from inspection of the curves in Figs. 1–4 for $n\leq 50$. By definition,[6]

$$\gamma_1=\mu_3/\sigma^3, \tag{5}$$

where μ_n is the nth moment of the distribution about the mean. A negative γ_1 means that the tail of the distribution for $S<\bar{S}$ is longer than the forward tail for $S>\bar{S}$. If $\gamma_1>0$ the opposite is true and $\gamma_1=0$ for the normal distribution. A measure of how the shape of the density function $f(S;n)$, in the vicinity of the mode, differs from that for the normal density function is given by the coefficient of excess[6]

$$\gamma_2=\mu_4/\sigma^4 \tag{6}$$

listed in Table III. If $\gamma_2<0$, $f(S;n)$ is more flat in the vicinity of the mode than the normal density function and more peaked if $\gamma_2>0$. In this regard $\gamma_2<0$ for the sp and sc lattices but $\gamma_2>0$ for bcc and fcc lattices. This suggests that γ_1 is independent of the lattice coordination number z but that $\gamma_2<0$ for $z\leq z_0$ where $6\leq z_0<8$.

A χ^2 test was used to judge the over-all fit of a normal distribution to the Monte Carlo data. The averages of the χ^2 values obtained using 21 deg of freedom (23 intervals) are given in Table IV over 500–900 jumps, 1000–5000 jumps, and 5000–10 000 jumps for each lattice. A composite average for the bcc and fcc distributions appears in the last column. According to Evans,[5] for example, given 21 deg of freedom, χ^2 in the range $13\leq\chi^2\leq 30$ indicates that the data at hand is very probably described by the assumed distribution, i.e., the normal distribution in this case. On the other hand, either $\chi^2<10$ or $\chi^2>36$ indicates that it is very unlikely that the data represents a randomly drawn set of values from the assumed distribution. Excepting the sp lattice, χ^2 decreased with increasing n for $n>500$. All χ^2 values were in the plausible fit range $10\leq\chi^2\leq 36$ for $n>1000$. Both the distribution for the sc lattice and that for the bcc lattice exhibited χ^2 values within the

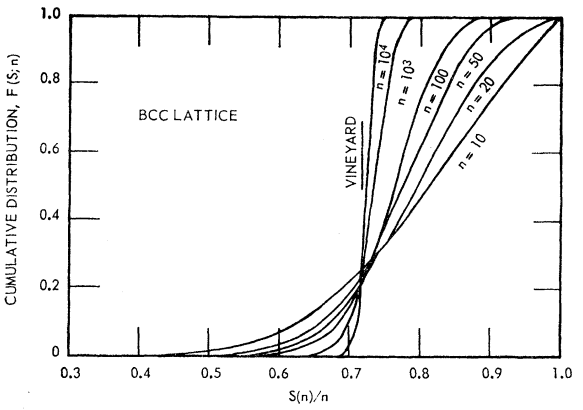

FIG. 3. Distribution function for bcc lattice.

TABLE I. Values of C in $\bar{S}(n)=B+Cn$ given by (a) 1000-history Monte Carlo (MC) calculations at $n=10^4$ and (b) Vineyard's exact solution for $n\rightarrow\infty$.

	(a) Monte Carlo ($n=10^4$)	(b) Vineyard ($n\rightarrow\infty$)	(a)/(b)
sc	0.6641	0.6595	1.005
bcc	0.7216	0.7178	1.005
fcc	0.7472	0.7437	1.005

TABLE II. Coefficient of skewness (γ_1) for Monte Carlo distributions $F(S;n)$.

	Skewness			
n	SPL	SCL	BCC	FCC
10	−0.054	−0.386	−0.558	−0.663
50	+0.07	−0.286	−0.320	−0.550
100	+0.003	−0.333	−0.364	−0.444
500	−0.130	−0.270	−0.540	−0.300
1000	−0.159	−0.238	−0.418	−0.293
2000	−0.230	−0.350	−0.40	−0.330
3000	−0.440	−0.330	−0.28	−0.320
4000	−0.400	−0.310	−0.26	−0.300
5000	−0.320	−0.320	−0.19	−0.340
6000	−0.320	−0.350	−0.20	−0.340
7000	−0.300	−0.280	−0.19	−0.300
8000	−0.310	−0.230	−0.21	−0.260
9000	−0.370	−0.200	−0.20	−0.220
10 000	−0.382	−0.169	−0.19	−0.205

very probable range for $n \geq 6000$ jumps. Because γ_1 and γ_2 for the bcc and fcc distribution behave similarly above $n=1000$ we feel that a composite average of χ^2 for these two lattices may be meaningful. This composite average is listed in the right-hand column. The χ^2 test indicates: (1) $F(S;n)$ is not well approximated by the normal distribution for $n<1000$; (2) the normal distribution is a good approximation to $F(S;n)$ for $10^3<n<10^4$; (3) $F(S;n)$ is very probably normal for $n>10^4$ in the three-dimensional case.

A least-squares analysis gives the following results for $\bar{S}(n)$ and $\sigma(n)$ on the interval $10^2 \leq n \leq 10^4$:

$$\bar{S}(n)=B+Cn, \tag{7}$$

$$\sigma(n)=An^k. \tag{8}$$

Values for the constants A, B, C, and k appear in Table V.

4. EFFECT OF FLUCTUATIONS ON THE INITIAL ANNEALING RATE

The distributions described in the previous section were computed to supplement a separate analog Monte Carlo study on defect annealing in cubic crystallites containing up to 2×10^6 lattice sites. In order to obtain even approximate agreement between the initial annealing rate given by the analog Monte Carlo[7] calculations and that computed using $F(S;n)$, it was necessary to consider the effect of fluctuations in the initial defect concentration within the crystallite. In this section the number of mobile defects remaining after an average of n jumps per defect is computed analytically in two ways. In the first instance the defect encounter probability is computed using $F(S;n)$ and the average concentration over the crystallite; in the second, it is computed using $F(S;n)$ and the average concentrations in each of N_c noninteracting crystallite subvolumes populated according to the random distribution law for M_0 defects in N_c boxes of equal volume. The two expressions are then applied in a numerical example for $M_0=100$ initially mobile defects in a fcc crystallite containing 5×10^5 sites and the results compared with those obtained in the Monte Carlo solution for this system.

TABLE III. Coefficient of excess (γ_2) for Monte Carlo distributions $F(S;n)$.

	Excess			
n	SPL	SCL	BCC	FCC
10	−0.455	−0.355	−0.301	−0.055
50	−0.270	+0.120	−0.14	+0.12
100	−0.158	+0.103	+0.339	+0.216
500	−0.170	+0.210	+0.56	+0.150
1000	−0.048	−0.094	+0.388	+0.043
2000	−0.030	−0.01	+0.76	+0.29
3000	+0.028	−0.10	+0.40	+0.16
4000	+0.22	−0.08	+0.16	+0.21
5000	+0.35	+0.006	+0.13	+0.11
6000	+0.17	−0.10	+0.04	+0.27
7000	−0.05	−0.13	+0.07	+0.34
8000	−0.001	−0.20	+0.11	+0.39
9000	−0.05	−0.20	+0.13	+0.11
10 000	−0.059	−0.12	+0.13	+0.12
	Less slim		More slim	

TABLE IV. Average χ^2 values over Δn ranges indicated. χ_c^2 is the average of columns three and four.

Δn	sp	sc	bcc	fcc	χ_c^2
500–900	27.6	39.8	47.5	38.8	42.0
1000–5000	34.8	34.4	26.8	32.2	31.1
6000–10 000	33.0	22.1	24.7	32.2	26.3

A. Average Concentration Approach

Let there exist M_0 mobile defects randomly distributed on Σ lattice sites and M_c defects contained in randomly distributed stable, immobile defect clusters at time $t=0$. Assume that the sole mobile defect removal process is association with other defects at contact. A pair of defects will be taken as stable and immobile in this example. Further, assume that the association probability ϵ at contact is the same when one member of the contact pair is a cluster member as when both defects were mobile just before contact. M_n will denote the number of mobile defects remaining after n jumps per defect. Let $\alpha=1/\Sigma$. The probability

TABLE V. $\bar{S}(n)$ and $\sigma(n)$ given by a least-squares analysis of the Monte Carlo data.

	$\bar{S}(n)=B+Cn$		$\sigma(n)=An^k$	
	B	C	A	k
sp[a]	...	...	0.194	0.799
sc	16.27	0.6642	0.414	0.608
bcc	16.90	0.7217	0.385	0.604
fcc	15.84	0.7473	0.308	0.635

[a] $\bar{S}(n)=0.7648n^{0.8935}$.

[7] N. R. Baumgardt and J. R. Beeler, Jr., Bull. Am. Phys. Soc. 9, 294 (1964).

that a mobile defect will encounter a cluster member on the nth jump is

$$\alpha[M_c+M_0-M_{n-1}]p^*(S;n-1)f(S;n-1), \quad (9)$$

where $p^*(S;n-1)$ is the conditional probability for a defect visiting $(S+1)$ distinct sites on the $(n+1)$th jump provided it had visited exactly S distinct sites in n jumps. The probability that a mobile defect will contact another mobile defect is

$$\alpha[M_{n-1}-1]p^*(S;n-1)f(S;n-1). \quad (10)$$

Contact with a cluster leads to the removal of one mobile defect but contact between two mobile defect leads to a depletion of two mobile defects; hence, the difference equation for M_n is

$$M_n=M_{n-1}-\alpha\epsilon[M_c+M_0-M_{n-1}] \times\sum_{S=S_1(n-1)}^{S=S_2(n-1)}[M_{n-1}f(S;n-1)]p^*(S;n-1) -2\alpha\epsilon[M_{n-1}-1] \times\sum_{S=S_1(n-1)}^{S=S_2(n-1)}[M_{n-1}f(S;n-1)p^*(S;n-1)]. \quad (11)$$

By the definition of $f(S;n)$ the summation reduces to $M_{n-1}\langle p^*(n-1)\rangle$. Equation (11) leads to the differential approximation

$$dM/dn\cong-\alpha\epsilon M\langle p^*(n)\rangle[M+(M_c+M_0-2)]. \quad (12)$$

Integration gives

$$\ln[M/(M+M_c+M_0-2)]_0^n =-\alpha\epsilon(M_c+M_0-2)\int_0^n\langle p^*(n)\rangle dn. \quad (13)$$

Collecting terms, one obtains

$$M(n)=M_0[M_c+M_0-2]/\{[2(M_0-1)+M_c] \times\exp[\alpha\epsilon(M_c+M_0-2)P_n]-M_0\}, \quad (14)$$

where $P_n=\int\langle p^*(n)\rangle dn$. Because $\langle p^*(n)\rangle$ is closely approximated by $d\bar{S}(n)/dn$, we will use

$$P_n=\int_0^n[d\bar{S}/dn]dn=\bar{S}(n). \quad (15)$$

$M(n)$ was evaluated for the particular case $\alpha=2\times10^{-6}$, $M_0=100$, $M_c=0$, and $\epsilon=1$. The results are discussed in Sec. 4C.

B. Consideration of Fluctuations

In the estimation of $M(n)$ outlined above one considered (M_c+M_0) defects in a cell of Σ sites and computed the contact probability from the average concentration

$$\bar{C}=(M_c+M_0)/\Sigma \quad (16)$$

TABLE VI. Probability $g(k)$ to find k defects in a subvolume of 5000 sites when the macroscopic defect concentration is $\bar{C}=2\times10^{-4}$ defects per site. $\bar{C}_k$ is the associated cell average concentration.

k	$g(k)$	$\bar{C}_k\times10^4$
0	0.366032	0
1	0.369730	2
2	0.184865	4
3	0.0609992	6
4	0.0149417	8
5	0.00289778	10
6	0.0046345	12

defects per site. The effect of fluctuations in the initial defect concentration upon the annealing rate can be estimated by introducing the density function $g(k)$ for finding exactly k mobile defects $(k=1,2,\cdots,M_0)$ in a given subvolume of a collection of N_c equal subvolumes with atomic-scale linear dimensions. Let $\tilde{M}(n)$ be the number of mobile defects remaining after n jumps, computed on the basis of $\{g(k)\}$ rather than $\bar{C}$, and set $M_c=0$. $\tilde{M}(n)$ then is

$$\tilde{M}(n)=\sum_{k=1}^{M0}M_k(n). \quad (17)$$

The quantity $M_n(k)$ is obtained by substituting $M_{0k}=kg(k)N_c$ for M_0, and $\alpha_k=1/g(k)\Sigma$ for α, in Eq. (14). The result is

$$M_k(n)=M_{0k}(M_{0k}-2)/\{2(M_{0k}-1) \times\exp[\alpha_k\epsilon(M_{0k}-2)P_n]-M_{0k}\}. \quad (18)$$

$\tilde{M}(n)$ was evaluated for the particular case $\alpha=2\times10^{-6}$, $M_0=N_c=100$ and $\epsilon=1$, using[8]

$$g(k)=M_0!(N_c-1)^{M_0-k}/k!(M_0-k)!N_c^{M_0}. \quad (19)$$

Values of $g(k)$ for $k\leq6$ are given in Table VI along with the associated subvolume concentrations. The average value $\langle k\rangle=1$ corresponds to an average concentration of 2×10^{-4} defects per site over the entire crystallite, the concentration used in computing $M(n)$.

C. Comparison with Monte Carlo Solution

In Fig. 5, $M(n)$, $\tilde{M}(n)$ and Monte Carlo solution, $M_{mc}(n)$, are compared for $\alpha=2\times10^{-6}$, $M_0=N_c=100$, and $\epsilon=1$ for $n\leq1000$. We will assume that M_{mc} is a physically more realistic solution than either M or $\tilde{M}$ because one would expect that it better describes the association of initially closely spaced defects. It will be used as the reference in all discussion. The curves become nearly parallel at $n=500$, and although it is not shown in the figure, they remained nearly parallel up to $n=2000$, the point at which the Monte Carlo runs were terminated. It appears, therefore, that dM/dn is

[8] W. Feller, *An Introduction to Probability Theory and Its Applications* (John Wiley & Sons, Inc., New York, 1957), 2nd ed., p. 34.

a good approximation to the true annealing rate for $n>500$ even though M itself is too large. Rapid association of defects, initially closely spaced, accounts for the more rapid falloff in $M_{\rm mc}$ for $n<500$ relative to that exhibited by M and $\tilde{M}$. The Monte Carlo method enables one to easily describe the removal of these initially close defects during the early annealing stage, a process only crudely described by $\tilde{M}$. It would seem that a rigorous analytical description of fluctuation effects in the association of randomly walking defects on a lattice would be somewhat complicated.

If one accepts $M_{\rm mc}$ as being more realistic than either M or $\tilde{M}$, our results indicate that the use of M in interpreting defect removal data would cause one to overestimate the number of jumps per defect required to attain a given removal fraction.[9] Table VII lists the number of jumps $n(M)$ and $n(M_{\rm mc})$ given by M and $M_{\rm mc}$, respectively, required to remove a given fraction of mobile defects. Extrapolation of the straight line log-log plot of $n(M)/n(M_{\rm mc})$ versus the removal fraction, gave a limiting value of ~ 1.1 for this ratio. In a strict sense, the ratios listed in Table VII should be regarded as lower bounds, especially when they are associated with $n>1000$. Although each defect was initially contained within a cube of 5×10^5 sites, in the Monte Carlo calculations, some defects migrated out of the cube into a defect-free environment during the annealing process. These escaping defects served to increase Σ a maximum of 2.4% at $n=1000$, i.e., a maximum of 1.2×10^4 sites outside the 5×10^5 site cube were visited. This caused $dM_{\rm mc}/dn$ to be slightly smaller

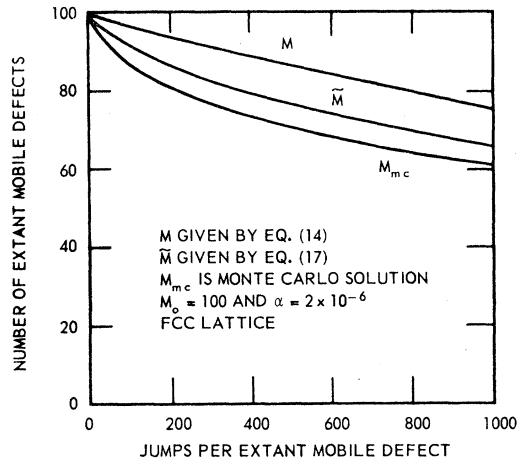

FIG. 5. Comparison of extant number of mobile defects after n jumps as given by M, $\tilde{M}$, and $M_{\rm mc}$ for a fcc lattice.

[9] After completion of this article, experimental evidence supporting this conclusion was found in a paper by F. Dworschak, K. Herschbach, and J. S. Koehler, Phys. Rev. 133, A293 (1964).

TABLE VII. Comparison of the number of jumps $n(M)$ and $n(M_{\rm mc})$ per extant mobile defect, given by M and $M_{\rm mc}$, respectively, required to remove a given fraction of mobile defects when $M_0=100$ and $\alpha=2\times10^{-6}$.

Fraction removed	$n(\tilde{M})$	$n(M_{\rm mc})$	$n(M)/n(M_{\rm mc})$
0.1	340	60	5.7
0.2	770	200	3.8
0.3	1350	520	7.6
0.4	2300	1070	2.2
0.5	3300	2000	1.6
1.0	...	...	~1.1

than it would have been had all defects remained inside the 5×10^5 site cell. At $n=2000\Sigma$ was increased a maximum of 3.5% by escaping defects.

Twenty-five Monte Carlo runs of 2000 jumps per extant mobile defect were made to obtain $M_{\rm mc}$. Five independent runs were made for each of five independent, randomly sampled initial defect distributions in a cube of 5×10^5 sites. A χ^2 analysis of the five initial distributions showed that they were consistent with the density function $g(k)$ of Eq. (19).

5. SUMMARY

The calculations described above indicate:

(1) $F(S;n)$ is not well approximated by the normal distribution for $n<5000$ jumps. However, $F(S;n)$ appears to approach the normal distribution on the interval $5000<n<10\,000$ and to be normal for $n>10^4$ in three-dimensional lattices.

(2) Our results give no conclusive evidence that $F(S;n)$ either does or does not approach the normal distribution in two-dimensional lattices.

(3) The use of Vineyard's asymptotic result for $\bar{S}(n)$, and the assumption that $F(S;n)$ is normal [using Table V for $\sigma(n)$] should give a very good approximation to the distribution of $S(n)$ for $n>10^4$.

(4) A computation of the mobile defect concentration and the *initial* annealing rate must account for the effect of fluctuations in the initial defect concentration.[9] Apparently, however, the annealing rate after the initial annealing stage can be well approximated by considering only the average defect concentration.

ACKNOWLEDGMENTS

The writer is indebted to Dr. G. H. Vineyard for communicating the results of his calculations in advance of publication and thereby suggesting the subject of the present article. J. A. Delaney and Miss N. R. Baumgardt wrote the computer programs used in this work.